Fast-Neutron Scattering from Nuclides in the Lead Region*

LAWRENCE CRANBERG
University of Virginia, Charlottesville, Virginia and University of California, Los Alamos Scientific Laboratory, Los Alamos, New Mexico

AND

THOMAS A. OLIPHANT AND JULES LEVIN
University of California, Los Alamos Scientific Laboratory, Los Alamos, New Mexico

AND

C. D. ZAFIRATOS
University of Colorado, Boulder, Colorado and University of California, Los Alamos Scientific Laboratory, Los Alamos, New Mexico

(Received 15 December 1966)

Experimental results and calculations are presented of an investigation of elastic and inelastic scattering of neutrons from bismuth and from separated isotopes of lead. Data are presented on spectroscopic properties of resolvable energy levels, excitation functions, nuclear temperatures, and angular distributions, with special emphasis on the application of the Wolfenstein-Hauser-Feshbach theory with width-fluctuation correction.

INTRODUCTION

IN this study of the scattering of fast neutrons from isotopes in the lead region, interest centers on spectroscopic information and on a quantitative study of the reaction mechanism in circumstances in which it is to be expected that compound-nucleus formation is the dominant process. Experimental conditions have been chosen which are favorable to the application of the statistical theory of nuclear reactions as formulated by Wolfenstein[1] and by Hauser and Feshbach,[2] (W-H-F) as amended[3] to include the effects of a correction due to fluctuation of level widths. To provide a basis for determining accurate values of the parameters of the optical model, so that the theory might be tested with a minimum of ambiguity arising from uncertainty in the parameters which enter into the calculations, data have been taken on elastic as well as inelastic scattering. The nuclides lead-206, -207, -208, and bismuth-209 were chosen because the experimental and theoretical information available on their level structures is considerable, although incomplete, and level structures of nuclides in the region of double-closed shells are of great intrinsic interest.

EXPERIMENTAL

The earliest versions[4] of pulsed-beam time-of-flight neutron spectrometers were suitable for application to a substantial range of problems of neutron-emission spectroscopy,[5] but were of limited value in meeting the more rigorous requirements of neutron-scattering spectroscopy. Where application was made to scattering, attention was focused on the statistical features of the observed spectra[6] or on the resolution of neutron groups corresponding to the excitation of individual states in the residual nucleus where such states were widely spaced—i.e., by energies of the order of several hundred keV or so.[7] With the apparatus described below, the energy resolution obtained in neutron scattering spectroscopy is in the range of 30 keV, and, by appropriate adjustment of the energy of the bombarding particle, this resolution can be realized at excitations up to 5 MeV in the residual nucleus. While this resolution falls short of what is obtainable by the methods of charged-particle spectroscopy, it has proven adequate for the scattering investigations reported here on isotopes in the lead region, where the effects of shell structure favor wide level spacing over a substantial range of excitation energy, and resolution of all levels is not essential to the purposes of the investigation.

The experimental work reported here was done at Los Alamos Scientific Laboratory. Development of one of the key components of the system-namely, the device for producing suitable bursts of monoenergetic ions, took place over a period of almost a decade in three stages. First, the dc beam from the Van de Graaff accelerator was "chopped" by an external electrostatic deflector. Second, the beam was "chopped" in the high-voltage terminal of the accelerator. The measurements

* Supported in part by the U. S. Atomic Energy Commission and the National Science Foundation.

[1] L. Wolfenstein, Phys. Rev. **82**, 690 (1951).

[2] W. Hauser and H. Feshbach, Phys. Rev. **87**, 366 (1952).

[3] P. A. Moldauer, Phys. Rev. **123**, 968 (1961).

[4] For a summary of the earliest work, see L. Cranberg, in *Proceedings of the First International Conference on the Peaceful Uses of Atomic Energy, Geneva, 1955* (United Nations, Geneva, 1956), Vol. 4, p. 43. For a more recent review, see *Fast Neutron Physics*, edited by J. B. Marion and J. L. Fowler (Interscience Publishers, Inc., New York, 1960), especially Chap. IV A.

[5] R. Grismore and W. C. Parkinson, Rev. Sci. Instr. **28**, 245 (1957).

[6] G. K. O'Neill, Phys. Rev. **95**, 1235 (1954); D. B. Thomson, *ibid.* **129**, 1649 (1963).

[7] L. Cranberg and J. S. Levin, Phys. Rev. **103**, 343 (1956); C. O. Muelhause, S. D. Bloom, H. E. Wegner, and G. N. Glasoe, *ibid.* **103**, 720 (1956). In a favorable case, the resolution was pushed to about 50 keV. See L. Cranberg and J. S. Levin, *ibid.* **109**, 2063 (1958).

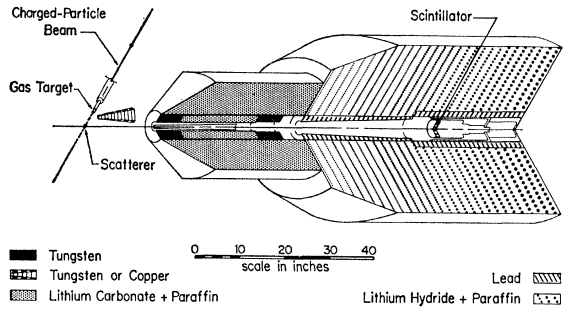

FIG. 1. Geometry of neutron spectrometer showing cutaway view of shield.

reported here were carried out with a third-stage apparatus,[8] in which a burst of ions of about 10-nsec duration produced by "chopping" in the terminal is effectively condensed in time by means of a so-called Mobley buncher. A further feature of the apparatus is the use of a detector 5 in. in diameter, in contrast to the 2-in.-diam detectors previously used, and a shield specially suited to the larger detector.

Details of the performance of a Mobley buncher very similar to the one used here have been given previously.[9] The essential features which distinguish the buncher used in this work from that previously described is that the writing speed of the deflector system has been increased so that optimum bunching can be obtained for protons of 6 MeV and deuterons of about 8 MeV. Increased writing speed is due in large part to an increase from 10 MHz to 20 MHz in the frequency of the rf voltage driving the deflector plates.

With a pulse repetition rate of 2 MHz, the accelerator typically delivered an average current to the target of 2 to 4 μA, depending on accelerator energy and other circumstances, with a burst duration (full width at half-maximum) in the neighborhood of 0.8 nsec.

The detector plastic scintillator of 5 in. diameter was coupled to a single photomultiplier, Amperex type 58 AVP. The latter was enclosed in a lead shield of $1\frac{1}{2}$-in. thickness, which was in turn enclosed by a mixture of LiH and paraffin 15 in. thick (see Fig. 1). As in previous work,[7,8] a wedge close to the target and a shield at a distance intermediate between wedge and detector were also used. A time-to-amplitude converter (TAC), followed by a 400-channel pulse-height analyzer, provided a record on punched tape of the time spectra. The latter were processed on an IBM 7090 to provide numerical data in a form convenient for summing and for determining the statistical accuracy of the counts in any group of consecutive channels.

To minimize time-slewing associated with variations in pulse height, a zero-crossing tunnel-diode circuit[10] with tunnel-diode discriminator was placed between the photomultiplier and the TAC. The block-diagram also included the usual parallel fast-slow arrangement.

For reasons which are not altogether clear, the resolution obtained (full width at half-maximum) for γ rays was consistently better than for neutrons. The precise value of the resolution figure was somewhat dependent on bias setting despite measures taken to minimize such dependence. Representative figures for γ-ray detection were about 1.5 nsec, and for 8-MeV neutrons about 2.0 nsec. At neutron energies in excess of 1 MeV, the energy resolution obtained was usually dominated by the instrumental time resolution. In general, as the energy of the scattered neutron diminishes, effects of geometry and of spread in energy of neutrons from the source begin to dominate the minimum resolution width. These effects became apparent at 1-MeV neutron energy and below, where the observed time spreads corresponded, typically, to an energy spread of about 30 keV, which could be accounted for on the basis of the following considerations.

Neutrons were produced by the $T(p,n)$ and $D(d,n)$ reactions using gas-targets. The gas was separated from the vacuum system by molybdenum foil 0.0001 in. thick. Straggling of the charged-particle beam in traversing the foil was typically about 20 keV, which accounted for a spread of about 20 keV in the energy of the neutrons at the scattering samples. This effect, together with contributions arising from the finite thickness of the target, and from the kinematics of the source reaction over the finite solid-angle subtended by the scatterer at the target, plausibly account for the observed resolution.

The lead and bismuth scattering samples were cylindrical, 1.6 cm in diameter, by 1.9 cm long, with an axial hole 0.15 cm in diameter so that they could be strung on a movable wire for easy handling. Each weighed about 50 g. Sample-to-scatterer distance was typically about 8 cm, and sample-detector distance was typically about 2.0 m. The samples of lead-206, -207, and -208 used in this work were electromagnetically separated by Oak Ridge National Laboratory. They were more than 99% pure except the sample of lead-207, which contained 4.7% 208 and 2.5% 206. Other samples used in this work were of natural isotopic composition.

Most of the angular distributions reported here were obtained with relative accuracies of three to ten percent, depending on the strength of a particular neutron group and the ease with which it could be resolved from adjacent groups. Normalization of an angular distribution to a scale of cross section per unit steradian introduced errors which are not included in the errors shown on the figures, except for the case of Fig. 11 for elastic scattering, where the errors shown include the uncertainty in normalization. Normalizations were obtained in all cases by comparison with the n-p scattering cross section, using thin polyethylene scatterers,

[8] The first results reported with this apparatus are given in L. Cranberg, C. D. Zafiratos, J. S. Levin, and T. A. Oliphant, Phys. Rev. Letters **11**, 341 (1963).

[9] L. Cranberg, R. A. Fernald, F. S. Hahn, and E. F. Shrader, Nucl. Instr. Methods **12**, 335 (1961).

[10] P. Orman, Nucl. Instr. Methods **21**, 121 (1963).

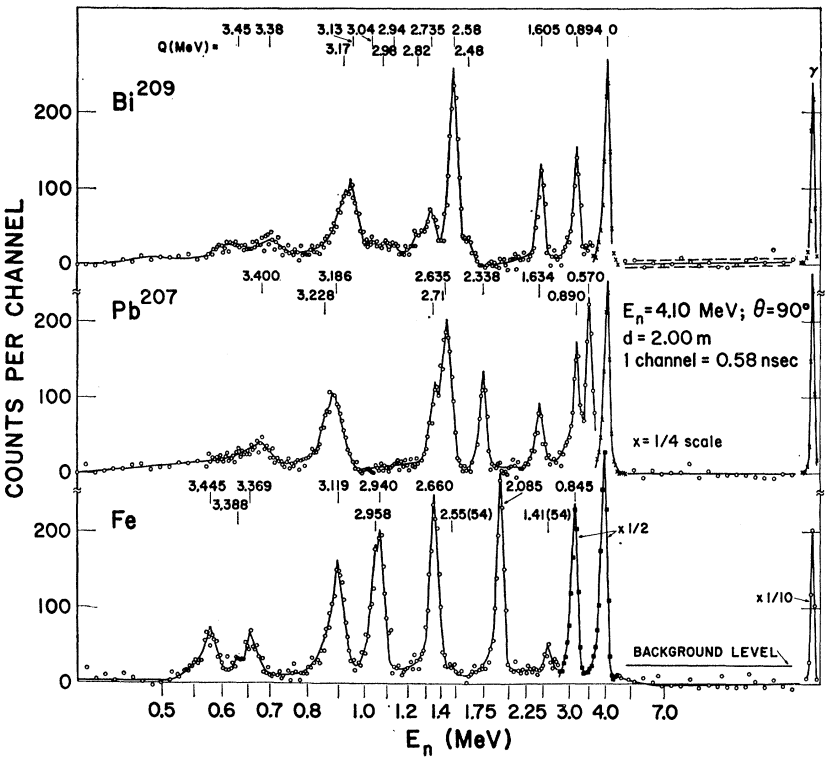

FIG. 2. Spectra observed for scattering of neutrons of 4.1-MeV energy from samples of Fe, Pb^{207}, and Bi^{209} under conditions shown in the figure. The dashed lines on the upper right part of the figure represent the statistical uncertainty associated with individual points in that portion of the data. The solid line in the lower right portion of the figure represents the magnitude of the "sample-out" background, which was essentially time invariant. In the iron spectrum all states observed are attributed to the predominant isotope of mass 56, except for two weak lines indicated by (54), attributed to iron-54, whose abundance in natural iron is 5.8%.

assuming an angular distribution for n-p scattering corresponding to isotropy in the center-of-mass system. This procedure is less direct and less accurate for elastic scattering than for inelastic scattering. In the important case of elastic scattering illustrated in Fig. 11, errors could be reduced, however, by subtracting the measured inelastic data from the known total cross section to give an independent check on the normalization of the measured angular distribution.

Corrections were made for isotopic purity of the lead samples and for attenuation by the samples, using methods previously described.[11] Corrections for multiple scattering were made only for the elastic scattering data; for inelastic scattering they are assumed to be small because of the near-isotropy of the results.

To minimize the kinematical, attenuation, and multiple scattering effects in the polyethylene, the samples were typically less than 0.4 cm in diameter, weighing about 0.33 g.

ENERGY LEVELS

Information on the positions, spins and parities of the nuclear levels studied here was incompletely known at the onset of the investigation. An initial purpose, therefore, was to identify the states in these nuclei which had already been reported and to determine what heretofore unreported states might be observable.

The most favorable conditions for observation of a particular state were obtained when the group of inelastically scattered neutrons corresponding to it had an energy between 0.7 and 1.0 MeV. Figure 2 shows representative spectra taken for an incident neutron energy of 4.1 MeV. The spectrum for natural iron is included to facilitate fixing the energy scale by reference to levels in iron-56 which are well known[12] from the results obtained by (p,p'). Figure 3 shows a family of spectra obtained for an incident energy of 3.5 MeV. Comparison of the spectra for lead-207 for the region of excitation corresponding to the neighborhood of 2.6 MeV, for the incident energies shown in Figs. 2 and 3, indicates the importance of adjusting the incident energies to achieve conditions most favorable for resolving a particular line.

Figure 4 shows the results inferred for the energy levels in lead-206, -207, and -208 and in bismuth-209. Excitation energies given to 1 keV are from previous work.[13] Those given to 10 keV are as observed in this investigation. All spins and parities are as determined by previous investigators, or, in the case of the 1.6-MeV state in bismuth, as predicted by the shell model.

As is evident from Fig. 2, the data on bismuth indi-

[11] L. Cranberg and J. S. Levin, Los Alamos Scientific Laboratory Report No. LA-2177, 1959 (unpublished).

[12] W. W. Buechner and A. Sperduto, quoted in *Nuclear Data Sheets*, compiled by K. Way *et al.* (Printing and Publishing Office National Academy of Sciences—National Research Council, Washington 25, D. C.) NRC 59-4-58.

[13] For data see *Nuclear Data Sheets*, compiled by K. Way *et al.* (Printing and Publishing Office National Academy of Sciences—National Research Council Washington, D. C., 1965); for Pb^{206} see NRC 61-4-110, for Pb^{207} see NRC 61-3-112, for Pb^{208} see NRC 61-3-126, and for Bi^{209} see NRC 5-3-88 (1963). The sheet on Bi^{209} includes the data published here for the first time.

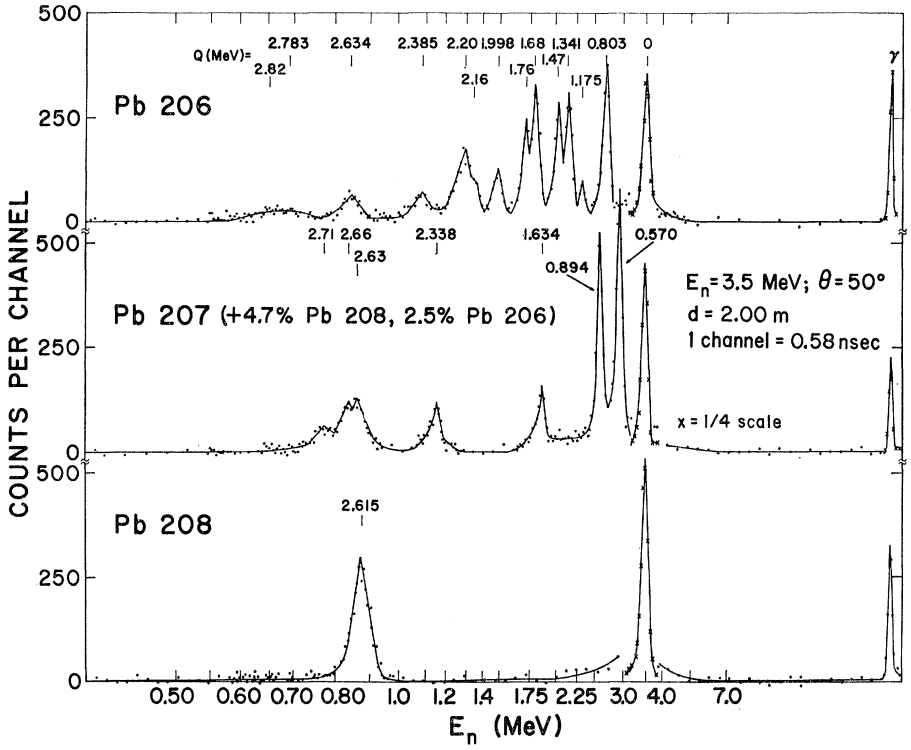

FIG. 3. Spectra observed for scattering of neutrons of 3.5-MeV energy from samples of Pb^{206}, Pb^{207}, and Pb^{208}. Correction to the spectrum of Pb^{206} due to the 4.7% contamination of Pb^{208} is not significant.

cate a large number of states incompletely resolved in the range of excitation energy above 1.6 MeV. The states indicated above that excitation energy for bismuth in Fig. 2 and 4 must, therefore, be taken as having only tentative significance.

Of particular interest are the three states resolved in lead-207 at 2.63, 2.66, and 2.71 MeV. The state at 2.71 MeV is plausibly identified with the state of 2.74 MeV reported previously[14] as being the $g_{9/2}$ single-particle state. The states at 2.63 and 2.66 MeV are plausibly identified as the doublet predicted by the discussion of de Shalit.[15] That discussion suggests that the octupole vibration, which is already well established[16] at 2.6 MeV in the lead region, might be nondegenerate with respect to coupling to the single neutron hole in the $p_{1/2}$ shell in lead-207. A weak coupling model therefore predicts a closely spaced doublet at 2.6 MeV in lead-207 with spins of $\frac{5}{2}$ and $\frac{7}{2}$.

Recently published work[17] strongly indicates that the state at 2.63 MeV is the $\frac{5}{2}$ state and the one at 2.66 MeV is the $\frac{7}{2}$ state. It is evident in our results that the three states under discussion are excited with progressively diminishing intensity despite the fact that they probably correspond to progressively increasing spins. We infer, therefore, that the relative cross section for excitation of these states is dominated by barrier penetration effects rather than the effect of statistical weight. The weak-coupling model also predicts splitting of the octupole state in the case of bismuth into seven components having spins from $\frac{3}{2}$ to 15/2. The strong intensity associated with the peak at 2.58 MeV in Fig. 2 suggests that the states in bismuth predicted by the weak-coupling model are unresolved in that figure. The large number of other states observed in bismuth in the energy range from 2.48 to 3.45 may be ascribed to breakup of the core.

In the absence of spin assignments, the several states in lead-206 and lead-208 reported here which have been heretofore unreported do not allow of interpretation on the basis of present evidence.

States in lead-207 at 1.98 MeV reported excited by the (d,p) reaction[18] and at 1.81 MeV excited by the (p,p') reaction[19] are not confirmed by our results. As will be seen later in this paper, nuclear excitation by (n,n') at our energies goes almost entirely via the compound-nucleus mechanism, and is not substantially affected by the single-particle versus collective character of the states. Excitation cross sections depend only on the excitation energy and on the spin of a state. Thus, failure to observe a state which is energetically accessible could be attributed to its high angular momentum. Since a state at 1.6 MeV is readily observed even though its spin is 13/2, failure to observe a state at 1.9 MeV

[14] P. Mukherjee and B. L. Cohen, Phys. Rev. **127**, 1284 (1962).
[15] A. de-Shalit, Phys. Rev. **122**, 1530 (1961).
[16] See, for example, B. L. Cohen and R. E. Price, Phys. Rev. **123**, 283 (1961).
[17] J. C. Hafele and A. G. Blair, Bull. Am. Phys. Soc. **11**, 12 (1966).
[18] B. L. Cohen, S. May, and R. E. Price, Nucl. Phys. **20**, 360 (1960).
[19] B. L. Cohen and A. G. Rubin, Phys. Rev. **111**, 1568 (1958).

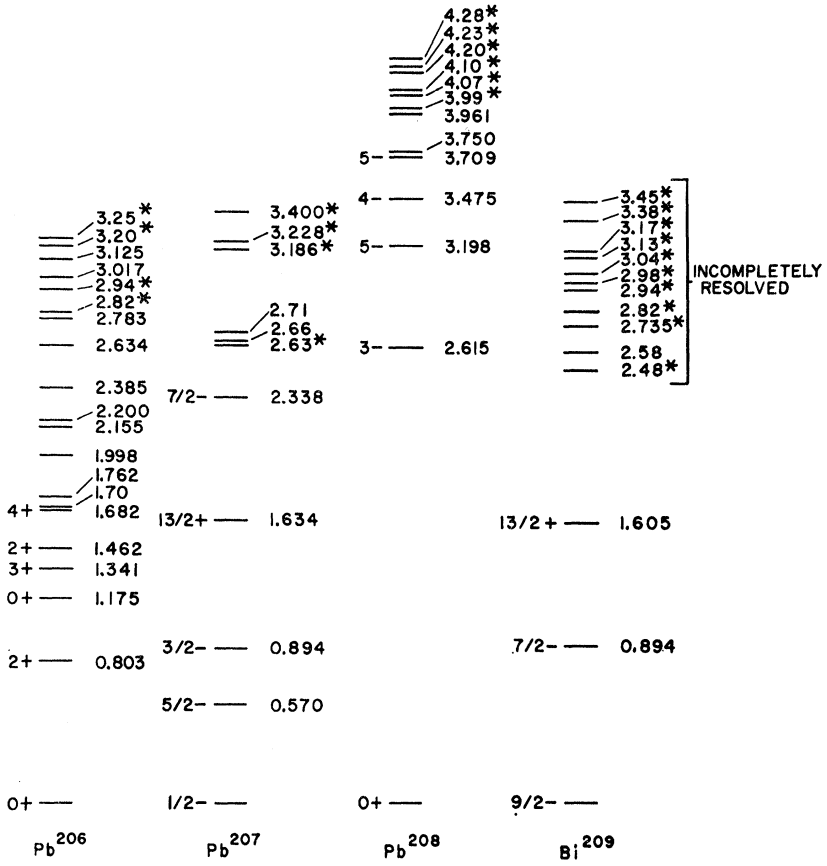

FIG. 4. Diagram of energy levels in Pb^{206}, Pb^{207}, Pb^{208}, and Bi^{209}. All energy levels marked with an asterisk are as inferred from this work; all others [*Nuclear Data Sheets* (Ref. 13)]. Spin and parities shown are those given [*Nuclear Data Sheets* (Ref. 13)] as firmly established, except for the 0+ excited state in Pb^{206} and the 13/2+ state in Bi^{209}. These are strongly suggested by this work and by the shell model (Ref. 30).

requires that if it exists its spin must be substantially greater than 13/2.

EXCITATION FUNCTIONS

Spectra were taken at a scattering angle of 50° at intervals of 0.25 MeV, for incident neutron energies from 2.0 to 5.0 MeV, and at 7.0 and 8.0 MeV. From these spectra, excitation functions were obtained for as many states as could be resolved. The results for lead-206 and lead-207 are shown in Figs. 5 and 6, respectively. Curves are drawn to facilitate identification of the points associated with the given state. The spins and parities shown on the figures are those known from previous work. The lead-206 data on which Fig. 5 is based were taken at the same intervals as those taken for lead-207, but the points have been omitted from Fig. 5 for the sake of clarity. In Figs. 5 and 6 the curves drawn from threshold to the first point at which an observation has actually been made are schematic only and are not based on any calculation.

These excitation functions indicate the qualitative features one expects for the trend of excitation functions generally in inelastic neutron scattering. At the energy threshold for excitation of a state, and for energies of 1 and 2 MeV above the threshold, the increasing ability of the emergent neutron to penetrate the nuclear potential barrier produces an initial rise in the cross section. With increasing bombarding energy, however, the opening up of increasing numbers of exit channels for decay of the compound-nucleus results in eventual monotonic decrease in the probability for exciting any individual state. The interplay of these two factors—i.e., competition and barrier penetration, account for the broad maxima which are a characteristic feature of most of the excitation functions.

The suggestions of dips in the excitation functions

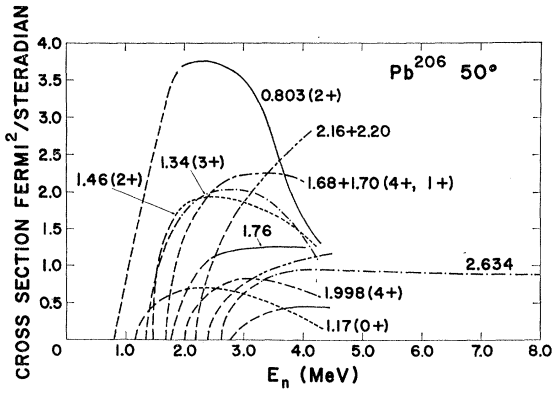

FIG. 5. Excitation functions for states resolved in Pb^{206} as observed at a scattering angle of fifty degrees.

TABLE I. Energy levels, spins, and parities assumed in reaction studies. All spins and parities, including values in brackets, are as given in *Nuclear Data Sheets* (Ref. 13), with the exceptions noted.

	Bi^{209}			Pb^{206}			Pb^{207}		
Level	Energy (MeV)	Spin	Parity	Energy (MeV)	Spin	Parity	Energy (MeV)	Spin	Parity
1	0	$\frac{9}{2}$	−	0	0	+	0	$\frac{1}{2}$	−
2	0.894	$\frac{7}{2}$	−	0.803	2	+	0.570	$\frac{5}{2}$	−
3	1.605	(13/2	+)[a]	1.175	(0	+)	0.894	$\frac{3}{2}$	−
4				1.341	3	+	1.634	13/2	+
5				1.462	(2	+)	2.338	$\frac{7}{2}$	−
6				1.682	4	+			
7				1.71	(1	+)			
8				1.762	(2	+)			
9				1.998	(4	+)			
10				2.155	(2	+)[b]			
11				2.200	(2	+)[c]			
12				2.200	(7	−)			
13				2.385	(6	−)			

[a] Suggested by shell model (Ref. 30).
[b] Trial value adopted in absence of prior assignment.
[c] Trial value adopted in view of qualitative inconsistency of assignment of 7 − with the observed excitation strength of the 2.200-MeV state.

for the two lowest-lying states of lead-207 at a bombarding energy of 3 MeV, if real, could be attributed to competition from a strongly excited state of 2.6 MeV. But errors of about ±10% associated with each point warrant caution. The dip at 2.25 MeV for the case of the second excited state is less reliably indicated. The relatively low maxima observed for the highest and lowest spin states are plausibly attributed to predominance of the role of the angular-momentum barrier and statistical weight, respectively.

A notable exception to the general rule of decreasing probability of excitation with increasing neutron energy is observed in the case of the 2.6-MeV states in Figs. 5 and 6. These clearly correspond to the 3- state which is excited predominantly by a process of direct interaction at the higher bombarding energies.[19] Observations of the detailed aspects of the direct interaction process for the 2.6-MeV state have been reported previously.[20]

Quantitative fitting of the observed excitation functions has not been attempted here. Qualitative considerations alone, however, indicate that the tentative assignment[13] of 7− to the state at 2.200 MeV state is inconsistent with the strong excitation of this state relative to the state at 2.15 MeV, as shown in Fig. 3, and with the magnitude of the excitation function for the two states combined as shown in Fig. 5. For this reason, in the work reported later in this paper, where quantitative analysis is attempted which requires an assumption for the spin of the state at 2.200 MeV, it has been assumed that there is a 2+ state in addition to a 7− at the same energy (see Table I).

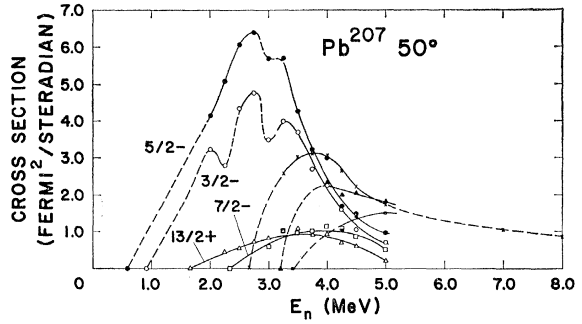

FIG. 6. Excitation functions for states resolved in Pb^{207} as observed at a scattering angle of 50°.

[20] L. Cranberg and C. D. Zafiratos, Phys. Rev. **142**, 775 (1966).

NUCLEAR TEMPERATURES

At energies in excess of about 6 MeV, only those states may be readily resolved which are preferentially excited by a direct process. Almost all others merge into a continum which may be analyzed only for its statistical features. Figure 7 represents a simplified analysis of the continuous portion of the neutron spectrum observed for lead-207 at a scattering angle of 90° for a bombarding energy 8.0 MeV. In this figure

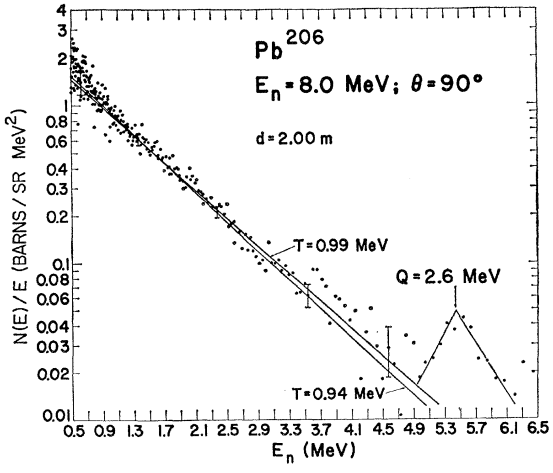

FIG. 7. The spectrum observed at a scattering angle of ninety degrees for Pb^{206}, for an incident neutron energy of 8 MeV, analyzed in terms of nuclear "temperature." Straight lines drawn correspond to values of the temperature shown in the figure.

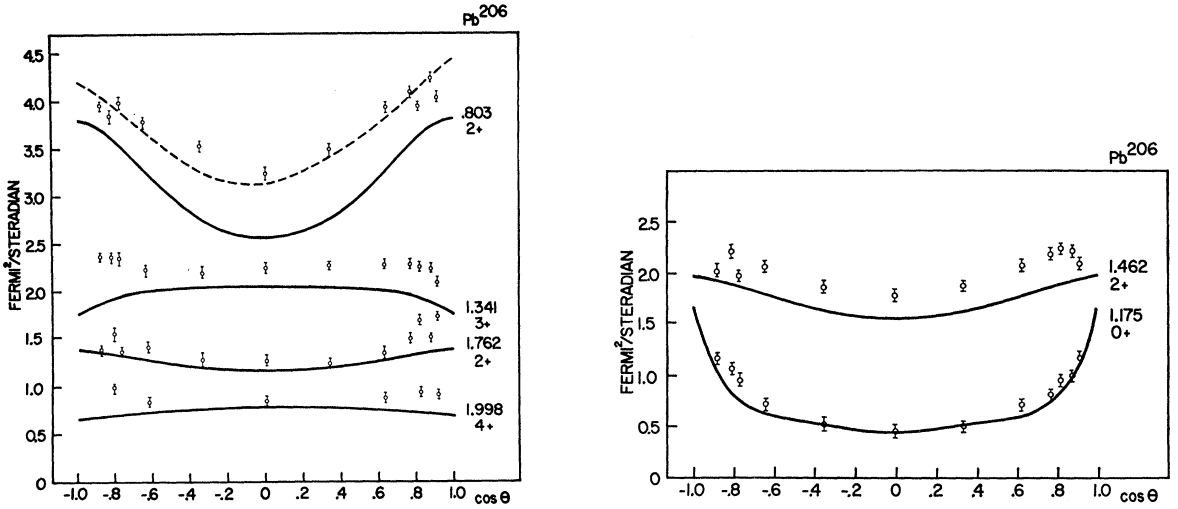

FIG. 8. Angular distributions of inelastically scattered neutrons corresponding to excitation of states in Pb^{206} shown on the figure for incident neutrons of 2.5 MeV. Solid lines are the results of Hauser-Feshbach calculations. The dashed line includes the effect of direct interaction for the 0.803-MeV state.

$N(E)/E$ is plotted semi-logarithmically versus energy E, of the emergent neutrons, where $N(E)$ is the number of emerging neutrons per unit energy interval. Straight lines are drawn corresponding to "temperatures" of 0.99 and 0.94 MeV, where the temperature is defined by the relationship: $-T=E\{\ln[N(E)/E]\}^{-1}$. The values obtained here for the temperature are consistent with those inferred previously[21] from data taken with lower energy resolution. It is clear in this figure that there is conspicuous excess above the statistical continum at an excitation energy of 2.6 MeV corresponding to the octupole state. This corresponds to the "high-energy excess" recorded in the work of Thomson.[21]

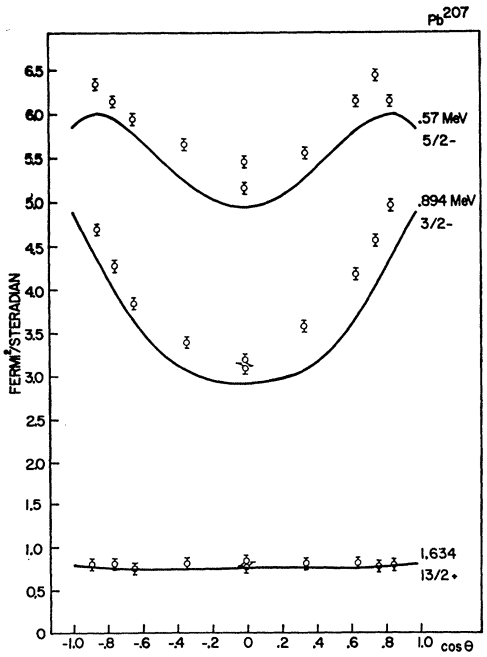

FIG. 9. Angular distributions of inelastically scattered neutrons corresponding to excitation of states in Pb^{207} shown on the figure, for incident neutrons of 2.5 MeV. Solid lines are the results of calculations as explained in the text.

ANGULAR DISTRIBUTIONS AT 2.5 MeV

An investigation was carried out of the angular dependence of inelastic neutron scattering in the lead region for incident neutrons whose energy is 2.5 MeV. This bombarding energy is one at which all, or almost all of the states which can be excited in these nuclei can also be reasonably well resolved, so that quantitative data can be obtained over a wide range of observation angles for the excitations of many of the states.

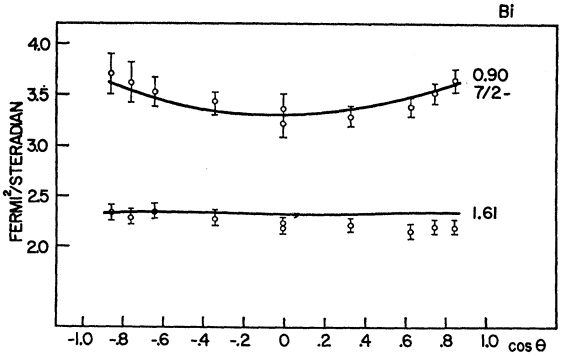

FIG. 10. Angular distributions of inelastically scattered neutrons corresponding to excitation of states in Bi^{209} shown on the figure, for incident neutrons of 2.5 MeV. Solid lines are the results of calculations as explained in the text.

[21] D. Thomson, Phys. Rev. 129, 1649 (1963).

TABLE II. Optical-potential parameters.[a]

	V (MeV)	W (MeV)	W_s (MeV F)	V_{so} (MeV F^2)	r_{01} (F)	a_1 (F)	r_{02} (F)	a_2 (F)
1. Best over-all	−46.35	+0.03	8.1	32	1.247	0.639	1.265	0.33
2. Best elastic	−46.05	+0.5	11.7	23	1.25	0.65	1.25	0.47
3. Previous (Ref. 22)	−41.86	0	3.60	20.8	1.32	0.635	1.32	0.635

[a] Potential: See Eq. (7) of Appendix.

Spectra illustrating the results obtained at a few representative angles for lead-206 have been reported previously and will not be reproduced here. The results of an earlier analysis of the data have also been reported previously.[22]

Figures 8, 9, and 10 illustrate the results obtained for the angular distributions of inelastically scattered neutrons from analysis of the spectra obtained as a function of angle for lead-206, lead-207, and bismuth-209. The errors include an estimate of the uncertainties associated with each point arising from the problems of subtracting proper backgrounds and resolving closely spaced states. In addition to the errors shown on each point, an estimated uncertainty of 5 to 7% is to be associated with the normalization for the points associated with a given state of excitation.

These data have been analyzed with the aid of the W-H-F theory as modified to include the effect of level-width fluctuations. The calculated results are shown as solid lines in Figs. 8, 9, and 10. In order to carry out this analysis it is essential to have reliable values for the transmission coefficients for ingoing and outcoming neutrons, and the energies, spins, and parities of all the states energetically accessible in the residual nuclei. Table I is an enumeration of the energies, spins, and parities of the states, as previously reported[13] up to an excitation energy of 2.5 MeV, which were used in the calculations.

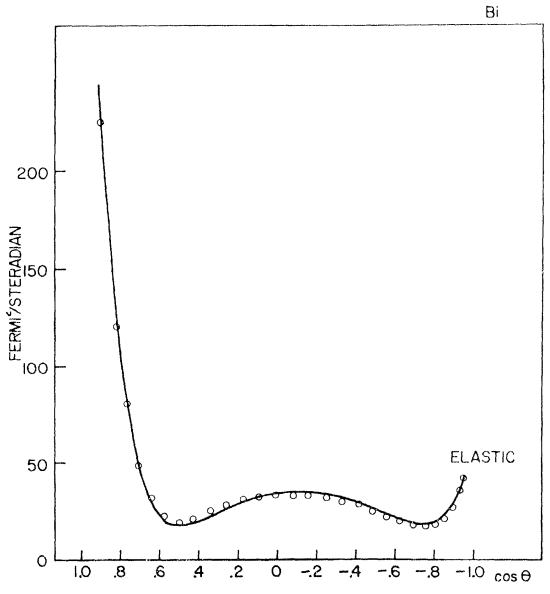

FIG. 11. Angular distribution of elastically scattered neutrons for 2.5-MeV neutrons incident on B^{209}. Solid line represents an optical-model fit to the data.

The assumption was adopted that the optical potential would be very similar for the three nuclides of interest, and that transmission coefficients could be appropriately calculated in all cases from an optical potential determined by fitting the data for one of them—namely, bismuth. Strong evidence for the similarity of the optical potentials of these nuclides has been adduced for 7-MeV neutrons.[23]

In order to determine the transmission coefficients for the W-H-F calculations with the greatest possible reliability and accuracy, a special set of data were obtained on elastic scattering for bismuth which is shown in Fig. 11. The relative errors associated with each point are estimated to lie within the diameter of each point, while the error in absolute values is estimated to be in the range of ±3%. These data have been corrected for multiple scattering by Monte Carlo methods. The optical model fit shown in Fig. 11 was obtained as described below, assuming the Perey-Buck[24] form for the optical potential (see Table II).

A search routine was applied in an extensive series of parameter searches to achieve a minimum value of χ^2. In this work, account was taken of the compound elastic as well as the inelastic scattering in bismuth, using W-H-F theory to achieve fits both to elastic and inelastic data. In carrying out this procedure the weights of the inelastic cross section of bismuth were multiplied by a factor of 10 to augment their effect in determining the best final fit. The series of searches which was carried out was extensive, including trial runs with and without the width-fluctuation effect, with and without separately adjustable radii for the real and imaginary portions of the optical potential, and with and without the extra weighting factor of 10 for the inelastic cross sections.

The quality of fit was systematically better with the width fluctuation effect, but was not appreciably affected by using different radii for the real and absorptive parts of the potential. Increasing the weight of the

[22] L. Cranberg, C. D. Zafiratos, J. S. Levin, and T. A. Oliphant, Phys. Rev. Letters **11**, 341 (1963).

[23] C. D. Zafiratos, T. A. Oliphant, J. S. Levin, and L. Cranberg, Phys. Rev. Letters **14**, 913 (1965).

[24] B. Buck and F. Perey, Nucl. Phys. **32**, 353 (1962).

inelastic cross sections by a factor of 10 degraded the quality of fit obtainable to the elastic data alone, but without the extra weighting factor inelastic results were too high. Inclusion of the extra weight factor gave the fit to the elastic scattering data shown by the solid curve in Fig. 11. The fits to the inelastic data obtained at the same time are as shown in Fig. 10. The parameters of the optical potential which gave the results shown in Figs. 10 and 11 are given in line one, Table II. Line two gives the parameters of the potential which gave an essentially perfect fit to the elastic data alone, but gave results about 10% too high for the 0.9-MeV state and about 20% too high for the 1.6-MeV state. Line 3 of Table II gives the parameters of the potential previously reported[22] for the best fit without the width fluctuation correction. With the parameters of line 1 in Table II, the solid curves shown in Figs. 8, and 9 were calculated for lead-206 and -207.

DISCUSSION OF ANGULAR-DISTRIBUTION DATA

It is clear that many of the leading features of the data are reproduced by the calculations. In general, symmetry about 90°, which may be taken as indication of consistency with the implication of the "statistical" assumptions of the theory, is clearly manifest within the limits of what may plausibly be claimed for the accuracy of the data. One of the most striking features of the results is the fidelity with which the calculations reproduce the shapes of the observed angular distributions, even where these differ little from one another as one goes from state to state.

Encouraged by the quality of systematic agreement exhibited by the data and the calculations, one is tempted to go one step farther and assign to the residual differences a genuine physical significance. This procedure is probably most warranted for the case of the 0.803-MeV 2+ state in lead-206, where the absolute magnitude of the cross section scale was checked with a special measurement, and the error is thought to be less than 5%, or only about one quarter of the discrepancy between experiment and the H-F calculation at 90°. Accordingly, a calculation of the effect of direct excitation of the 2+ state, supplied by Satchler,[25] was normalized to the difference between theory and experiment. In this theory the normalizing factor so obtained can be interpreted directly in terms of β, the deformation parameter. In Fig. 8, the dashed curve shows the sum of the H-F calculation and the direct contribution for a β of 0.07. This result may be compared with that reported by Alster,[26] inferred from inelastic α scattering, of 0.06 ± 0.012, and a value of $0.037_{-0.008}{}^{+0.004}$ inferred[27] from measured values of $B(E2)$.

[25] R. G. Satchler (private communication).
[26] J. Alster (private communication).
[27] P. H. Stelson and L. Grodzins, Nucl. Data **A1**, 33 (1965).

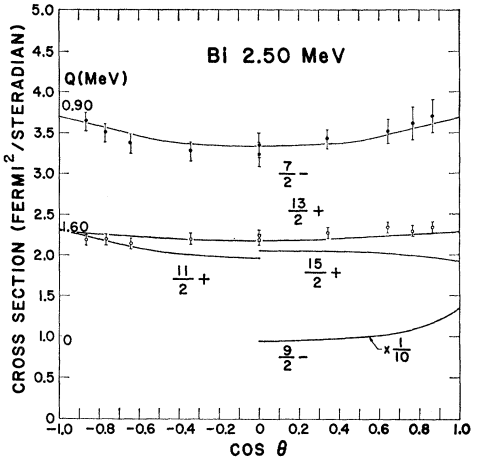

FIG. 12. Angular distribution of inelastically scattered neutrons corresponding to excitation of the excited states in Bi^{209}, together with calculated values for a range of assumed spins for the state at 1.6 MeV.

Simple addition of the direct and compound nucleus contributions is a procedure which may have no special theoretical sanction, but it is offered as a tentative way of treating the data. The agreement with Alster is consistent with this handling of the data.

It is tempting to suggest that other discrepancies of absolute magnitudes of cross sections may be similarly resolved, particularly because the calculated results are systematically somewhat lower than the observations. It is doubtful, however, that any firm significance can be attached to the remaining differences, in view of the uncertainties in the absolute cross section scale of the other angular distributions.

It is appropriate to note that in interpreting discrepancies between H-F calculations and experiment, one may adduce a possible dependence of optical-model parameters on the energy of the emerging neutrons. Such a dependence has been discussed on theoretical grounds[28] and some experimental data have been analyzed[29] by introducing such a dependence on an *ad hoc* basis. These analyses did not, however, include the role of width-fluctuation effect. In the present analysis there is considerably less need for an adjustment of the potential to individual levels, and none has been made.

Encouraged by this pattern of agreement, calculations were made for the case of bismuth-209 with a variety of choices for the spin and parity of the second excited state of that nuclide, and the results are shown in Fig. 12. The assignment of 13/2+ for that state seems reasonably assured on the basis of the shell model.[30] From Fig. 12 we see that 11/2, 13/2, and

[28] G. L. Shaw, Ann. Phys. (N. Y.) **8**, 509 (1959); L. C. Gomes, Phys. Rev. **116**, 1226 (1959).
[29] D. A. Lind and R. B. Day, Ann. Phys. (N. Y.) **12**, 485 (1961).
[30] See, for example, J. Blomquist and S. Wahlborn, Arkiv Fysik **16**, 545 (1959-60).

15/2 give appreciably different shapes, albeit with small anisotropies in each case. The data are in best agreement with calculations for a spin of 13/2, although the agreement of absolute magnitude for the 13/2 case was forced in the fitting procedure and cannot be regarded as significant. It may be noted that the results calculated for different choices of parity in a number of randomly selected cases showed little sensitivity to parity, so that the results of Fig. 12 must be interpreted as being significant at most with respect to the assignment of spin.

CONCLUSION

Most significant of the results reported here is the consistency with which the W-H-F theory predicts experimental results for angular distributions of inelastically scattered neutrons for a wide range of spins at a neutron energy of 2.5 MeV. The quality of the agreement is significantly improved by incorporation of the width fluctuation factor. In one case a significant residual difference between theory and experiment can be interpreted in terms of direct interaction. Information on positions of nuclear energy levels for nuclei in the lead region are extended to excitation energies of about 4 MeV, but the result for a previously reported state at 1.9 MeV in lead-207 is negative.

ACKNOWLEDGMENTS

The development effort incidental to the research program described here was the work of many persons and institutions, some of whose contributions have been acknowledged in previous publications. It is particularly appropriate here, however, to express appreciation of the engineering skill of R. E. Fernald and the executive judgment of Denis Robinson of the High Voltage Engineering Corporation, for reducing to practice the principle of ion-bunching suggested by R. C. Mobley and R. J. Van de Graaff, including modifications of the earliest design which permitted extension to higher particle energies. Thanks are due, as always, to Dr. J. L. McKibben and the operating staff of the Los Alamos Van de Graaff accelerator for their support. The ready and expert technical assistance of H. J. Lang was continuously valuable. Finally, it is a pleasure to record appreciation of discussions of the weak-coupling model with Dr. J. J. Griffin.

APPENDIX

We have analyzed our data in terms of Hauser-Feshbach theory[1,2] and in terms of this theory as it has been recently modified by Moldauer.[3] According to the Hauser-Feshbach theory, the differential cross section for the inelastic scattering of unpolarized neutrons from an unpolarized target nucleus can be written in the following form

$$\frac{d\sigma}{d\Omega}=\frac{\pi}{(2s+1)(2I+1)k^2}\sum_{J p_c}\sum_{ll'jj'}(2l+1)\Lambda_l(p,p_c)\times\Lambda_{l'}(p',p_c)\frac{T_{lj}T_{l'j'}}{D(\mathrm{J},p_c)}\times\sum_{m_s m_s' M_I M_I'}\{C(lsj;0,m_s)\times C(l's'j';m_l',m_s')C(jIJ;m_s,M_I)\times C(j'I'J;m_j'M_I')\times\left[\frac{(2l'+1)}{4\pi}\frac{(l'-|m_l'|)!}{(l'+|m_l'|)!}\right]^{1/2}P_{l'}^{m'l}(\theta)\Big\}^2, \quad (1)$$

The Γ and Γ' refer, respectively, to the state of excitation of the target before and after the scattering. In all our calculations our target will be assumed to be initially in its ground state. We denote the neutron spin ($\frac{1}{2}$) by by the letter s and the spin of the target nucleus as I (before collision) or I' (after collision). k is the incident wave number in F^{-1} so that the differential cross section will be given in F^2. The parity operator $\Lambda_l(p,p_c)$ is defined by

$$\Lambda_l(p,p_c)=\tfrac{1}{2}[1+(-1)^{l+p+p_c}]. \quad (2)$$

Here l is the orbital-angular-momentum quantum number, p is the parity of the target nucleus, and p_c is the parity of the compound nucleus. We have used l and p (l' and p') for the before (after) collision values. The quantities T_{lj} and $T_{l'j'}$ are the incident and decaying partial wave transmission coefficients. The denominator $D(J,p_c)$ is given by

$$D(J,p_c)=\sum_{l''j''\Gamma''}\Lambda_{l''}(p'',p_c)T_{l''j''}(\Gamma'')\delta_{Jj''I''}. \quad (3)$$

The Γ'' sum indicates a sum over all energetically possible final target excitations. p'' refers to the parity of the target state Γ''. The sum over l'', j'' goes over all partial waves for each target state Γ''. The $\delta_{Jj''I''}$ factor represents the triangular relation

$$\delta_{Jj''I''}=1 \text{ if } |j''-I''|\leq J\leq|j''+I''|$$
$$=0 \text{ otherwise}. \quad (4)$$

The sum on j'' goes from $l''-\frac{1}{2}$ to $l''+\frac{1}{2}$. The C's are the Clebsch-Gordan or Wigner coefficients discussed fully by Rose.[31] $P_{l'}^{m_{l'}}(\theta)$ is the usual associated Legendre polynomial. If we integrate over θ, we obtain for the total inelastic cross section for $\Gamma\rightarrow\Gamma'$, the expression

$$\sigma(\Gamma,\Gamma')=\frac{\pi}{(2s+1)(2I+1)k^2}\sum_{J p_c}\sum_{ll'jj'}(2J+1)\Lambda_l(p,p_c)\times\Lambda_{l'}(p,p_c)\frac{T_{lj}T_{l'j'}}{D(J,p_c)}. \quad (5)$$

[31] M. E. Rose, *Elementary Theory of Angular Momentum* (John Wiley & Sons, Inc., New York, 1957).

The transmission coefficients T_{lj} and $T_{l'j'}$ obtained by solving the Schrödinger equation with a suitable optical potential

$$\frac{d^2u}{dr^2}+\left[k^2-\frac{l(l+1)}{r^2}-\frac{2mV_{\text{opt}}(r)}{\hbar^2}\right]u=0. \tag{6}$$

The wave number k in F^{-1} is given in accordance with the incident center-of-mass energy for the T_{lj} and the incident center-of-mass energy minus the final target excitation energy for the $T_{l'j'}$. m is the reduced mass in amu and $\hbar^2$ is given in MeV F^2 amu. The optical potential is in MeV. The optical potential is written as follows:

$$V_{\text{opt}}(r)=(V+iW)f_1(r)+iW_s\frac{df_2(r)}{dr}+V_{so}\frac{\langle\mathbf{l}\cdot\mathbf{s}\rangle_\pm}{r}\frac{df_1(r)}{dr}, \tag{7}$$

where the shape factors $f_i(r)$ are given by

$$f_i(r)=\left[1+\exp\left(\frac{r-r_{0i}A^{1/3}}{a_i}\right)\right]^{-1}. \tag{8}$$

The V will be a negative constant. The W will be a small constant for most of our results and may have either sign. The W_s will be the dominating imaginary factor and since the derivative will already have a minus sign in it, W_s will be positive. It will be in units of MeV F. The constant V_{so} will be in MeV F^2. The factor $\langle\mathbf{l}\cdot\mathbf{s}\rangle_\pm$ is the only factor depending on whether $j=l\pm s$. Its value is given by

$$\langle\mathbf{l}\cdot\mathbf{s}\rangle_+=l/2, \qquad \langle\mathbf{l}\cdot\mathbf{s}\rangle_-=-(l+1)/2. \tag{9}$$

We could choose different optical potential parameters depending on the state of excitation of the target nucleus. However, this would give too many parameters to make any sense in a fit and we have at present no sensible way to make any postulates on what the difference should be.

Now let us indicate Moldauer's modification of the theory. In (1) and (5) above, the following factor appears:

$$\frac{T_{lj}T_{l'j'}}{D(J,p_c)}.$$

Since the denominator is a sum over T's we write this factor briefly as follows:

$$T_iT_{i'}/T, \tag{10}$$

where $T=\sum_{i''}T_{i''}$. Moldauer gives three basic corrections.[3]

(1) The transmission coefficients T_j should be replaced by the strength functions τ_j.

(2) The expression (10) must be multiplied by a correction factor $R_{ii'}$ which we will write below.

(3) Higher-order terms should be added.

If we use (2) without (1) or (3), flux is still conserved and our answer is meaningful. However, to use (1) in a flux-conserving way, we must also consider (3) which is beyond our present means. Hence, we only use (2). Therefore our "Moldauer modification" consists of the following replacement:

$$\frac{T_iT_{i'}}{T}\rightarrow\frac{T_iT_{i'}}{T}R_{ii'}. \tag{11}$$

The correction factor $R_{ii'}$ can be written

$$R_{ii'}=\int_0^\infty dt\frac{1}{[1+(2+T_i)/T][1+(2+T_{i'})/T]}\times\prod_k\left[\frac{1}{1+(2tT_k)/T}\right]^{1/2}. \tag{12}$$

We have used the following expression for χ^2:

$$\chi^2=\frac{1}{N}\sum_c\sum_i\left(\frac{\sigma_{\text{th},c}(\theta_i)-\sigma_{\text{exp},c}(\theta_i)}{\Delta\sigma_{\text{exp},c}(\theta_i)}\right)^2W_c, \tag{13}$$

where

$$N=\sum_c\sum_i 1. \tag{14}$$

Here $\sum_c$ represents the sum over the various elastic and inelastic scattering processes. The $\sum_i$ represents the sum over the angles for a given elastic or inelastic scattering process. If we set $W_c=1$, we obtain the usual χ^2 which is used in fitting. However, we found that it was desirable to increase the weights W_c by a factor of 10 for the inelastic scattering processes in order to obtain better over-all fits to all the competing processes. This is mainly because of the relatively small number of inelastic scattering data points compared to the large number of elastic scattering data points.

We obtained our fits to the data by varying the indicated parameters, in the examples discussed below, in such a way as to minimize the χ^2 given in (13). The computer program we used for this purpose was adapted from a program written by J. Wills while at this laboratory.